Pflugers Arch - Eur J Physiol (2003) 446:695–701
DOI 10.1007/s00424-003-1118-8

ION CHANNELS, TRANSPORTERS

Haruko Masumiya · Hiroto Tsujikawa · Naoki Hino · Rikuo Ochi

Modulation of manganese currents by 1, 4-dihydropyridines, isoproterenol and forskolin in rabbit ventricular cells

Received: 29 March 2003 / Accepted: 20 May 2003 / Published online: 25 June 2003

Abstract Although often used as a Ca^{2+} channel blocker, Mn^{2+}, in fact, permeates through Ca^{2+} channels. Under Na^+-free conditions, depolarizing pulses evoked slowly-decaying Mn^{2+} currents (I_{Mn}). Maximal I_{Mn} densities in the presence of 5 and 20 mM Mn^{2+} were 0.42±0.12 pA/pF (mean±SEM, n=17) and 1.23±0.10 pA/pF (n=40), respectively. At 5 mM, the ratio of maximal amplitude of I_{Mn} to that of the Ca^{2+} current (I_{Ca}) was 0.079±0.009 (n=8). I_{Mn} elicited from a holding potential of −50 mV was depressed by nitrendipine (1 μM) by ~70%. Nitrendipine (0.3 μM) shifted the steady-state inactivation curve to more negative potentials and shifted the potential for half-maximal inactivation ($E_{0.5}$) from 1.3 to −8.8 mV and also decreased the time constant of decay of I_{Mn} at 20 mV from 986.2 to 167.9 ms. BAY K 8644 (1 μM), isoproterenol (10 μM) and forskolin (10 μM) all increased I_{Mn} and shifted the current/voltage (I/V) relationship to more negative potentials. The small, slowly-inactivating I_{Mn} is thus modulated by dihydropyridine Ca^{2+} channel modulators and cyclic AMP-mediated phosphorylation in a manner similar to other L-type Ca^{2+} channel currents. L-type Ca^{2+} channels are involved in the regulation of intracellular [Mn] in ventricular myocytes.

Keywords L-type Ca^{2+} channel · Manganese · Nitrendipine · BAY K 8644 · Isoproterenol · Forskolin

H. Masumiya · H. Tsujikawa · R. Ochi (✉)
Department of Physiology,
Juntendo University School of Medicine,
113-8421 Tokyo, Japan
e-mail: ochir@med.juntendo.ac.jp
Tel.: +81-3-58021028
Fax: +81-3-58021028

N. Hino
Institute of Physiology,
Juntendo Medical College of Nursing,
Urayasu, 279-0023 Chiba, Japan

Introduction

The L-type Ca^{2+} channel, which mediates the influx of Ca^{2+} that triggers contraction in cardiac muscle, is characterized by high voltage sensitivity, ion selectivity and pharmacological modulation [23]. The amplitudes and time courses of inactivation of macroscopic L-type Ca^{2+} channel currents have been characterized for Ca^{2+}, Ba^{2+}, Sr^{2+} and Na^+ [7]. The amplitudes of single-channel currents show a channel conductance profile of Na^+>Ba^{2+}>Sr^{2+}>Ca^{2+} [15]. The L-type Ca^{2+} current is blocked competitively by Cd^{2+}, Co^{2+}, Ni^{2+}, Mn^{2+}, Mg^{2+} and La^{3+} [11, 19], whereby blockade does not necessarily mean that the blocking ion is incapable of permeating through the channel [19]. For instance, both slow Mn^{2+}-dependent inwards currents [27] and propagated Mn^{2+}-dependent action potentials [28] have been recorded from guinea-pig ventricular muscle fibres using a hybrid technique entailing the combined application of single sucrose-gap and microelectrodes. Mn^{2+} currents, or related depolarizations, have also been recorded from excitable cells other than cardiac myocytes, including insect muscles [9], myoepithelial cells from a polychaete worm [3] and snail neurons [2].

The trace element Mn in ionic form (Mn^{2+} or Mn^{3+}) is required for many essential cellular enzymes, making regulation of its intracellular concentration crucial for normal cell function [26, 34]. In that regard, several mechanisms for the transport of Mn^{2+} across the cell membrane have been identified: e.g. Na^+-Ca^{2+} exchange transports Mn^{2+} to the inside of red blood cells [8], Ca^{2+} and Mn^{2+}-permeable channels are activated by store depletion in various cells [29] and the widely expressed transient receptor potential channel (melastatin)-7 (TRPM7) channel mediates cellular entry of various trace metal ions, including Mn^{2+} [24]. In addition, because Mn^{2+} binds to voltage-gated Ca^{2+} channels more strongly than Ca^{2+}, those channels also mediate Mn^{2+} influx [4, 17], despite the fact Mn^{2+} permeates through them less readily than Ca^{2+}. In the present study, we characterized the voltage-gated Mn^{2+} current (I_{Mn}) in rabbit ventricular

myocytes and studied its pharmacological modulation. Mn^{2+} current density was much lower than that of the Ca^{2+} current (I_{Ca}) (8% at maximal current density); the currents inactivate slowly and are modulated by dihydropyridines; and are augmented by cAMP-related signal transduction.

Materials and methods

This study was conducted in accordance with the guiding principles for the care and use of animals in the field of physiological sciences set forth by the Physiological Society of Japan [31]. The protocol was approved by our University's Animal Experimentation Committee.

Ventricular cells

Single ventricular myocytes were isolated from rabbit hearts as described previously [18]. Briefly, Japanese white rabbits (1.6 kg) were anaesthetized by injection of pentobarbitone sodium (40 mg/kg) or urethane (1.25 g/kg) into the auricular vein, and the ascending aorta cannulated in situ under artificial respiration. The hearts were then excised quickly and perfused in the Langendorff mode for several minutes with Tyrode solution gassed with 100% O_2 and warmed to 37 °C to wash out the blood. They were then perfused with nominally Ca^{2+}-free Tyrode solution for 5 min, with collagenase solution for 25 min and with high-K^+ solution for 5 min. Thereafter, single cells were dissociated from the ventricles and stored in high-K^+ solution at 4 °C.

Patch clamp procedure

Membrane currents were recorded employing the whole-cell configuration of the patch-clamp technique [12] with an appropriate patch-clamp amplifier (Axopatch l-D, Axon Instruments, Foster City, Calif., USA). Patch pipettes were pulled from plain capillary tubes made of soda lime glass (Chase Instruments, N.Y., USA), coated with Silgard (Silpot 184, Dow Corning, Midland, Mich., USA) and heat-polished under a microscope. Pipette resistance was 2–5 MΩ when filled with pipette solution. The liquid junction potential between the pipette and normal Tyrode solution was corrected before seal formation. After formation of a gigaohm-seal, the pipette capacitance was compensated before membrane currents were recorded. The patch membrane was disrupted by applying negative pressure. Then, by applying 10-mV step pulses, whole-cell membrane capacitance was determined either from the peak amplitude and the time constant of decay or from the current integral of the capacitive transients. Series resistance was compensated and currents were filtered at 1 kHz and recorded at a sampling frequency of 5 kHz. Step-pulse protocols and data acquisition were carried out using pCLAMP software (Axon Instruments). Mn^{2+} current amplitude was estimated from the deflection of the maximal inwards current during depolarization steps from zero current (I=0). All experiments were conducted at room temperature (22–25 °C).

Solutions

Normal Tyrode solution contained (mM): NaCl 135, KCl 5.4, $CaCl_2$ 1.8, $MgCl_2$ 1.0, HEPES 5 and glucose 10 (pH 7.40 with NaOH). $CaCl_2$ was omitted from nominally Ca^{2+}-free solution. Collagenase solution contained 45 mg collagenase (Sigma, Type 1) in 50 ml of low (20 μM) Ca^{2+}-containing Tyrode solution. High-K^+ solution contained (mM): glutamic acid 70, oxalic acid 10, KCl 25, KH_3PO_4 10, HEPES 5, glucose 10, taurine 10 and EGTA 5 (pH 7.35 with KOH). The test extracellular solution contained (mM): tetraethylammonium chloride (TEA-Cl) 143, $MgCl_2$ 1, HEPES 5 and $MnCl_2$ 5, or $MgCl_2$ 4, or $CaCl_2$ 5 (pH 7.35 with TRIS). When the [$MnCl_2$] was increased to 20 mM, the TEA-Cl concentration was reduced to 121 mM. The pipette solution used to record Mn^{2+} currents contained (mM): *N*-methyl-D-glucamine (NMDG) 130, $MgCl_2$ 1, ATP-Mg 3, HEPES 5, EGTA 10 (pH 7.35 with TRIS). Nitrendipine was kindly provided by Dr. Jun Inui (Yoshitomi Pharmaceutical Co. Ltd. Japan). (±)BAY K 8644 and forskolin were purchased from Sigma (St. Louis, Mo., USA). BAY K 8644, forskolin and nitrendipine were dissolved in ethanol as 10 mM stock solutions. Isoproterenol was added to the Mn^{2+} solution immediately before application. All other drugs and chemicals were commercial products of the highest quality available.

Statistics

Data are presented as means±SEM. Data were analysed using Student's *t*-test for paired samples. $P<0.05$ was considered significant.

Results

Properties of I_{Mn}

I_{Mn} was evoked with 400-ms depolarizing pulses from a holding potential of −50 mV (Fig. 1A). In Mn^{2+}-free, 5 mM Mg^{2+} solution, the test pulses evoked no inwards currents, and only small outwards currents. In contrast, depolarizing pulses in the presence of 5 or 20 mM Mn^{2+} evoked sustained inwards currents. The time course of I_{Mn} was characterized by a slow rise and a slow decay at −20 or −10 mV. I_{Mn} amplitude increased with depolarization, reaching a peak at potentials of 10–30 mV and decreasing with further depolarization. The time courses of activation and inactivation accelerated with depolarization, shortening the peak time of the I_{Mn}.

The current-voltage (I/V) relationships of I_{Mn} were obtained by plotting the maximal inwards current density during a test pulse as a function of the membrane potential (Fig. 1B). In the presence of 5 mM Mn^{2+}, I_{Mn} was activated at −20 mV and gradually increased with further depolarization until 10 or 20 mV. The current then decreased with further depolarization, though inwards currents were still observed at 70 mV. In the presence of 20 Mn^{2+}, I_{Mn} appeared at −10 mV and its I/V curve crossed that obtained with 5 mM Mn^{2+} at 0 mV with the generation of larger inward currents. I_{Mn} increased gradually until 20 or 30 mV and decreased with further depolarization. However, a relatively large inwards current flowed at 70 mV. In the presence of 5 mM and 20 mM Mn^{2+}, maximal I_{Mn} density was 0.42±0.12 pA/pF (mean±SEM, n=17) and 1.23±0.10 pA/pF (n=40), respectively. We compared the density of I_{Mn} with that of Ca^{2+} current (I_{Ca}) at 5 mM. The maximal density of I_{Ca} recorded prior to I_{Mn} was 9.20±2.13 pA/pF (n=8), while that of I_{Mn} was 0.66±0.14 pA/pF. The ratio of maximal amplitude of I_{Mn} to that of I_{Ca} was 0.079±0.009 (n=8).

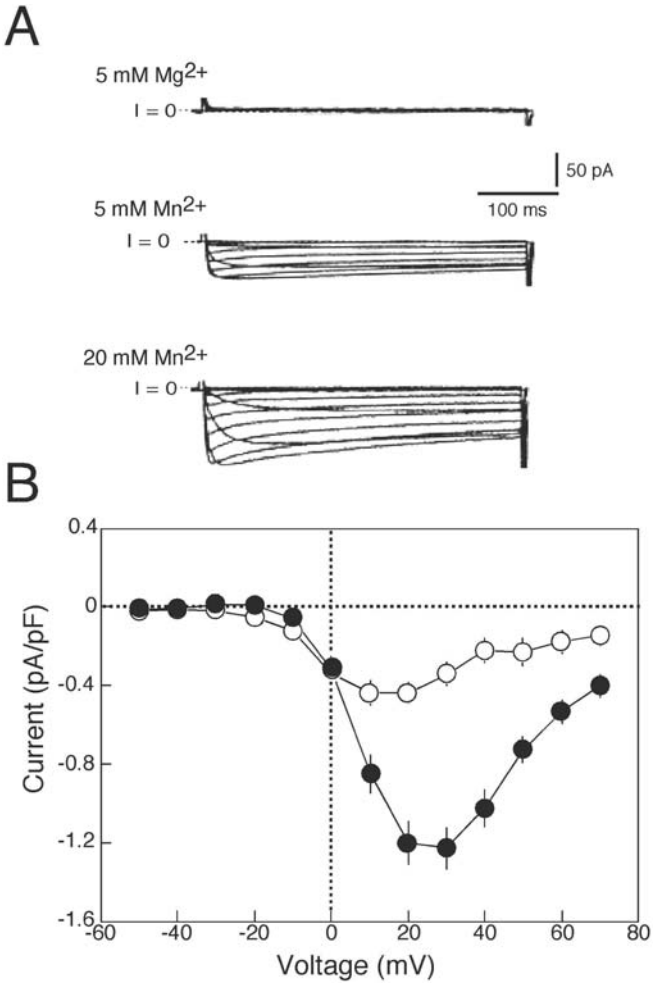

Fig. 1A, B Mn^{2+} currents (I_{Mn}) and current-voltage (*I/V*) relationships. Depolarizing steps with a duration of 400 ms were applied from a holding potential (HP) of −50 mV to 70 mV in 10-mV increments. **A** Superimposed current traces obtained in the presence of Mn^{2+}-free solution containing 5 mM Mg^{2+} (*uppermost panel*) or solution containing 5 (*middle panel*) or 20 mM Mn^{2+} (*lowest panel*). No inwards currents were elicited in Mn^{2+}-free solution. **B** *I/V* relationships of I_{Mn}. Maximal inwards deflection from I=0 in the presence of 5 (*open circles*, n=17) or 20 mM Mn^{2+} (*closed circles*, n=40) were plotted as a function of membrane potential. Means±SEM

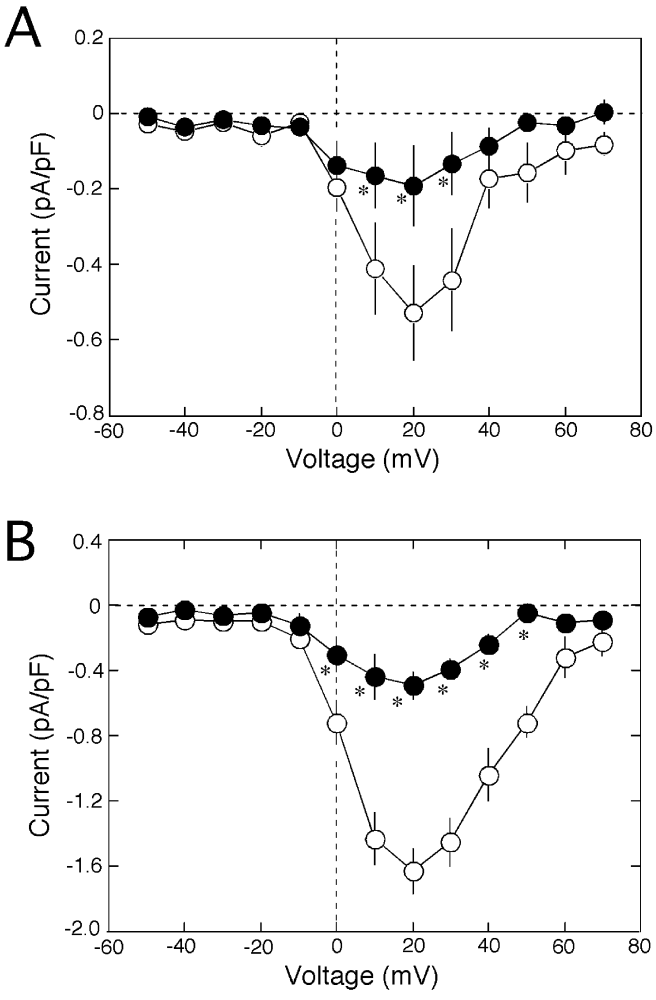

Fig. 2A, B Effects of nitrendipine on the *I/V* relationship of I_{Mn}. Current densities of I_{Mn} in the presence of 5 mM Mn^{2+} (**A**) or 20 mM Mn^{2+} (**B**), with (*closed circles*) or without (*open circles*) 1 μM nitrendipine, are shown as functions of membrane potential. The membrane potential was held at −50 mV and 400-ms test pulses to 70 mV in 10-mV increments were applied. Means±SEM, n=5 (**A**) or 6 (**B**) experiments; *P<0.05 vs. corresponding control

Effects of nitrendipine on I_{Mn}

The dihydropyridine Ca^{2+} channel blocker nitrendipine (1 μM) reduced the peak amplitudes of I_{Mn} activated by test pulses from a holding potential of −50 mV (Fig. 2). On average, nitrendipine reduced the maximal I_{Mn} in the presence of 5 or 20 mM Mn^{2+} by 69.2±13.9% (n=5) and 72.6±3.8% (n=6), respectively. Nitrendipine reduced inwards currents to about the same extent at all potentials.

Fig. 3 shows the effects of nitrendipine (0.3 μM) on the quasi-steady-state inactivation of I_{Mn} in the presence of 20 mM Mn^{2+}. The inactivation curve shows the dependence of I_{Mn} recorded at a test potential of 20 mV on the membrane potential during the preceding 1 s. Normalized I_{Mn} inactivation curves were well fitted by a Boltzmann equation: $I_{Mn}/I_{max}=1/\{1+\exp[(E_{max}-E_{0.5})/k]\}$, where I_{max} is the maximal I_{Mn} amplitude, $E_{0.5}$ the potential for half-maximal inactivation and k the slope factor. I_{max} was 1.73±0.23 pA/pF (n=10) under control conditions and 1.60±0.28 pA/pF in the presence of 0.3 μM nitrendipine. Exposure to nitrendipine shifted the inactivation curve to more negative potentials. As a result, $E_{0.5}$ shifted from 1.3 mV in the control to −8.8 mV in the presence of 0.3 μM nitrendipine, whereby k decreased slightly from −12.3 to −10.2.

Nitrendipine also accelerated the time course of I_{Mn} inactivation. Figure 4 shows that inactivation of I_{Mn} evoked by 1-s depolarizations to 20 mV in the presence of 20 mM Mn^{2+} was markedly accelerated by 0.3 μM nitrendipine. The time course of the decay of I_{Mn} was fitted by a single exponential curve with a time constant

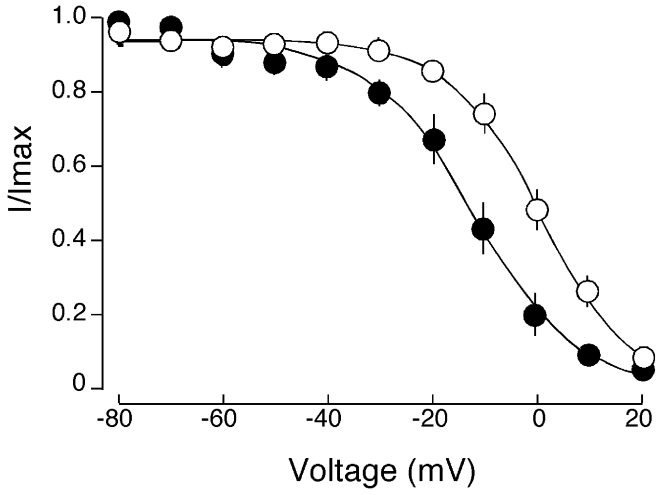

Fig. 3 Effect of nitrendipine on the steady-state inactivation of I_{Mn}. The steady-state inactivation curves were obtained in the presence of 20 mM Mn^{2+}, with (*closed circles*) or without (*open circles*) 0.3 μM nitrendipine. Membrane potential was held at −80 mV and currents evoked by test pulses to 20 mV following 1-s prepulses from the HP to 20 mV in 10-mV increments. I_{Mn} amplitude was normalized to the maximal amplitude and plotted as a function of the prepulse potential. The *solid lines* are the fits to the Boltzmann equation (see text)

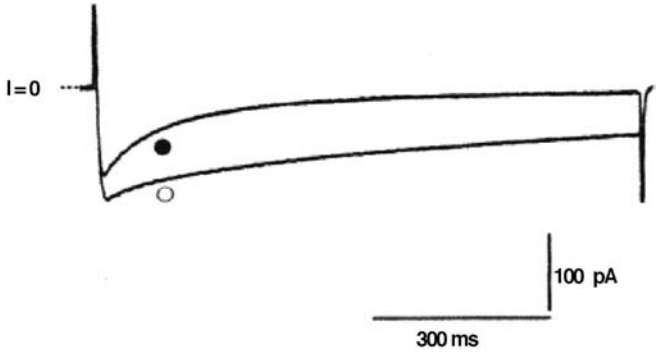

Fig. 4 Effect of nitrendipine (0.3 μM) on the time course of decay of I_{Mn}. External solution contained 20 mM Mn^{2+}. Currents were elicited by 1-s depolarizing test pulses to 20 mV from a HP of −80 mV. The time course of decay was fitted by monoexponential *curves* in the absence (*open circle*) and presence (*closed circle*) of nitrendipine

(τ) of 1,137 ms under control conditions and 164 ms in the presence of nitrendipine. On average, 0.3 μM nitrendipine shortened τ from 986.2±167.9 ms (n=6) to 167.9±13.0 ms.

Effects of BAY K 8644 on I_{Mn}

The dihydropyridine Ca^{2+} channel agonist BAY K 8644 (1 μM) increased the amplitude of I_{Mn} in the presence of 20 mM Mn^{2+} and accelerated the rate of inactivation (Fig. 5A). The *I/V* curves show that BAY K 8644 markedly increased I_{Mn} at 0 mV and shifted the relationship 10 mV toward more negative potentials (Fig. 5B). BAY K 8644 also increased maximum current density from 2.3±0.2 pA/pF at 30 mV (n=7) to 3.7±0.5 pA/pF at 20 mV. With depolarizations to greater than 30 mV in the presence of BAY K 8644, I_{Mn} gradually declined. At potentials greater than 40 mV, the amplitudes of I_{Mn} evoked in the presence and absence of BAY K 8644 were comparable, presumably because the open state probability was higher also under control conditions.

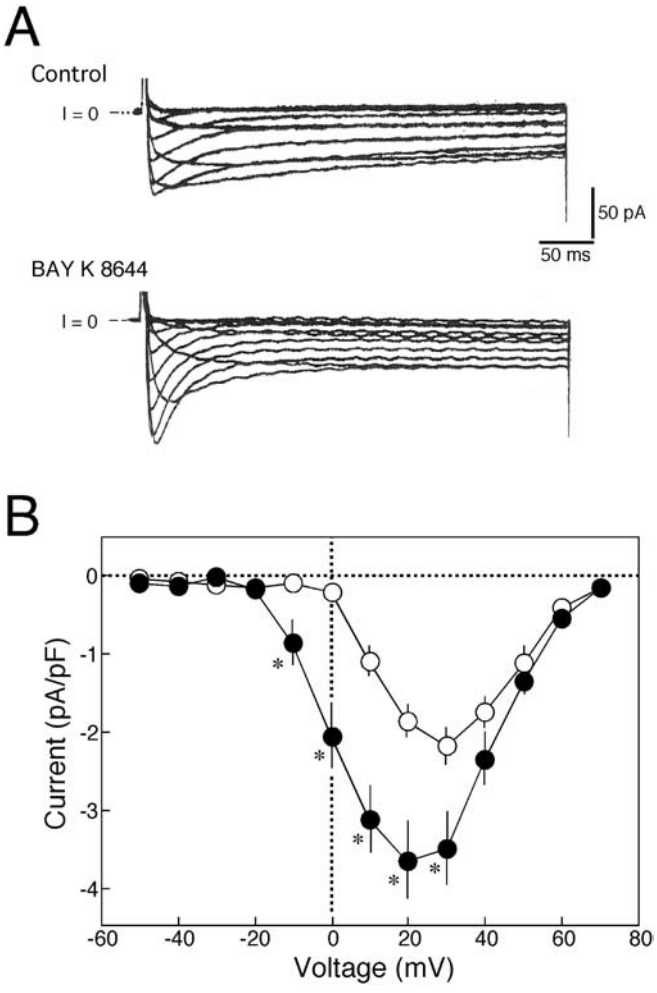

Fig. 5A, B Effects of BAY K 8644 on I_{Mn}. I_{Mn} was evoked in the presence of 20 mM Mn^{2+} by 400-ms depolarizing steps from a HP of −50 mV to 70 mV in 10-mV increments. **A** Superimposed current traces in the absence and presence of 1 μM BAY K 8644. **B** *I/V* relationships for I_{Mn} in the absence (*open circles*) and presence (*closed circles*) of 1 μM BAYK 8644. Means±SEM; n=7 experiments; *P<0.05 vs. corresponding control

Effects of isoproterenol on I_{Mn}

The representative traces in Fig. 6A show that I_{Mn} evoked by depolarizing pulses from a holding potential of −50 mV in the presence of 20 mM Mn^{2+} was enhanced

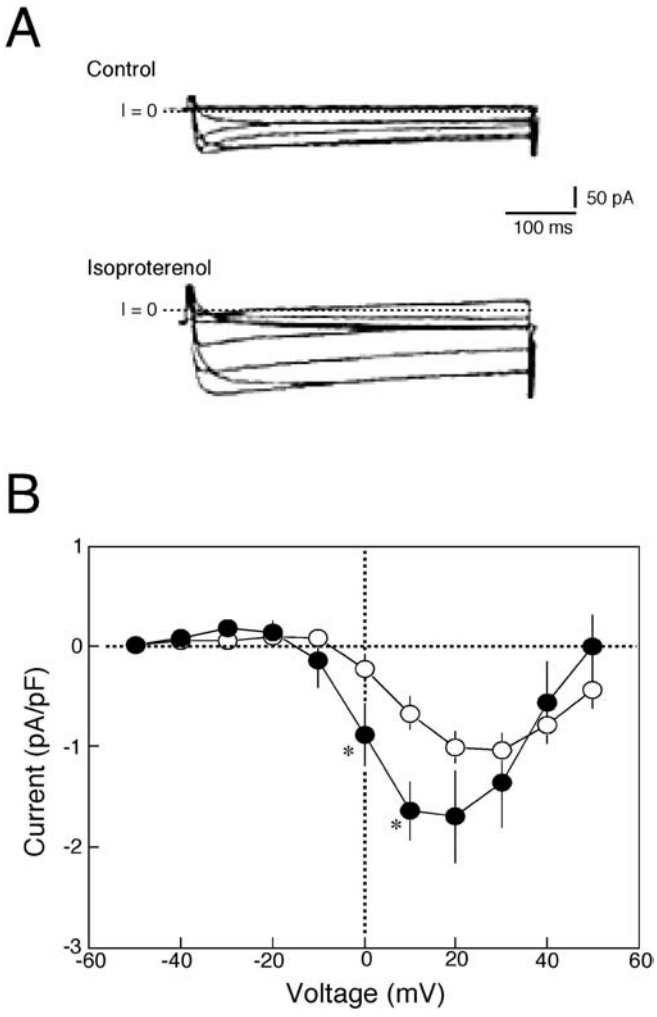

Fig. 6A, B Effects of isoproterenol on I_{Mn}. I_{Mn} was evoked in the presence of 20 mM Mn^{2+} by 400-ms depolarizing steps from a HP of −50 mV to 50 mV in 10-mV increments. **A** Superimposed current traces in the absence (*upper panel*) and presence (*lower panel*) of 10 μM isoproterenol. **B** *I/V* relationships for I_{Mn} in the absence (*open circles*) and presence (*closed circles*) of isoproterenol. Means±SEM; *n*=8 experiments; **P*<0.05 vs. corresponding control

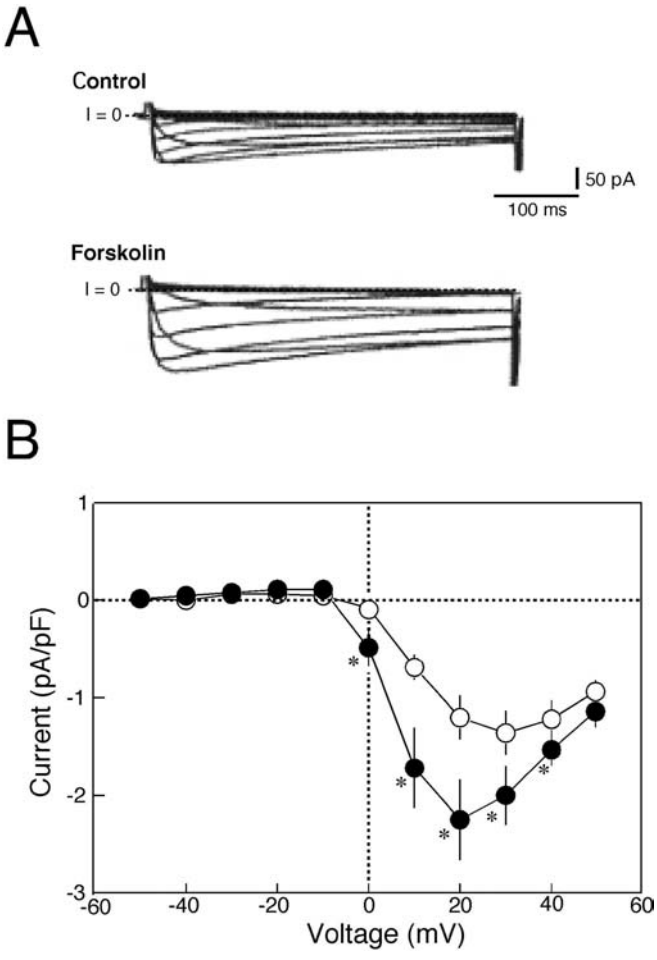

Fig. 7A, B Effects of forskolin on I_{Mn}. I_{Mn} was evoked in the presence of 20 mM Mn^{2+} by 400-ms depolarizing steps from holding potential of −50 mV to 50 mV in 10-mV increments. **A** Superimposed current traces in the absence (*upper panel*) and presence (*lower panel*) of 10 μM forskolin. **B** *I/V* relationships for I_{Mn} in the absence (*open circles*) and presence (*closed circles*) of forskolin. Means±SEM; *n*=7 experiments; **P*<0.05 vs. corresponding control

by 10 μM isoproterenol and that the enhancement was associated with a slight slowing of the time course of inactivation at strongly depolarized potentials. The *I/V* curves show that isoproterenol enhanced I_{Mn} and shifted the relationship by about 10 mV toward more negative potentials (Fig. 6B). Isoproterenol significantly increased I_{Mn} density from 0.65±0.11 to 1.82±0.29 pA/pF at 10 mV (*n*=8).

Isoproterenol often shifted the holding current at −50 mV slightly inwards and induced small outwards currents at large positive pulses (Fig. 6A). Furthermore, the *I/V* curve obtained in the presence of isoproterenol crossed the control curve at 40 mV, indicating that I_{Mn} declined more steeply with the increasing depolarization in the presence of isoproterenol. These changes are probably due to the activation of a sustained Cl^- current [13].

Effects of forskolin on I_{Mn}

As shown by the representative traces in Fig. 7A, forskolin (10 μM) enhanced I_{Mn} in the presence of 20 mM Mn^{2+} at all potentials. The enhancement was significant at potentials between 0 and 40 mV and the *I/V* relationship shifted towards more negative potentials (Fig. 7B). The maximal I_{Mn} density was increased by forskolin from 0.71±0.14 to 1.77±0.43 pA/pF at 10 mV (*n*=7).

Discussion

Small but distinct Mn^{2+} currents were elicited by depolarization of rabbit ventricular myocytes. These currents were depressed by nitrendipine and enhanced by BAY K 8644, isoproterenol and forskolin. Although small in amplitude, their voltage dependence and pharmacological sensitivity to dihydropyridines and activators of adenylate cyclase indicate that I_{Mn} reflects permeation of Mn^{2+} through L-type Ca^{2+} channels.

The activation and inactivation of I_{Mn} in the presence of 5 or 20 mM Mn^{2+} occurred at membrane potentials more positive than is seen with normal L-type Ca^{2+} currents. This is due probably to the high [Mn^{2+}] used to increase the amplitude of I_{Mn}, which would be expected to have a membrane stabilizing effect [5, 16]. To confirm that the I_{Mn} permeated through the L-type Ca^{2+} channel, we examined its sensitivity to highly selective dihydropyridine Ca^{2+} channel modulators [14]. Nitrendipine, a dihydropyridine Ca^{2+} channel blocker, depressed I_{Mn} without affecting the *I*/*V* relationship (Fig. 2), although the steady-state inactivation curve shifted in the negative direction (Fig. 3), consistent with the previously described voltage-dependent blockade of L-type Ca^{2+} and Ba^{2+} currents [18, 21, 37]. Nitrendipine also accelerated I_{Mn} decay during depolarization steps (Fig. 4), consistent with its binding to the channel in the open state [18]. BAY K 8644, a dihydropyridine Ca^{2+} channel agonist, increased I_{Mn} and shifted the activation curve to more negative potentials (Fig. 5), as has been seen previously with permeation of Ca^{2+} and Ba^{2+} through the L-type channels [10, 32]. In sum, the sensitivity of I_{Mn} to a dihydropyridine Ca^{2+} channel modulators confirms unequivocally that Mn^{2+} permeates through L-type Ca^{2+} channels as a charge carrier in rabbit ventricular cells.

The observed effects of isoproterenol and forskolin indicate that I_{Mn} was modulated also by cAMP-mediated phosphorylation in a manner similar to other cardiac L-type Ca^{2+} channel currents (Figs. 6, 7). Isoproterenol stimulates adenylate cyclase via Gsα, whereas forskolin stimulates the enzyme directly to increase the amplitude of I_{Mn} and produce the characteristic negative shift in the *I*/*V* relationship [23]. Thus, modulation of L-type Ca^{2+} channel behaviour via protein kinase A-mediated phosphorylation increased passage of Mn^{2+} through the channel just as it does with other permeable ions. Indeed, the observed retardation of the time course of I_{Mn} inactivation (Figs. 6 and 7) is analogous to the phosphorylation-dependent modulation of L-type Ba^{2+}, Sr^{2+} and Na^{+} currents [7]. Cyclic AMP also activates cystic fibrosis transmembrane conductance regulator (CFTR) Cl^{-} currents in cardiac muscle [13, 22]. In that regard, the observed increases in the inwards holding current and the intersection at 40 mV of the *I*/*V* curves obtained in the presence and absence of isoproterenol are explained by the generation of CFTR Cl^{-} currents (Fig. 6). The absence of a corresponding CFTR Cl^{-} current in the presence of forskolin (Fig. 7) might reflect the direct blockade of the channel by the drug, as it is known to directly affect various channel-currents [20].

The fact that permeant ions can act as blockers is well known. Ca^{2+} is potent inhibitor of monovalent ion current through the L-type Ca^{2+} channels [19]. A set of four glutamate residues (EEEE locus), located at homologous positions in each of the four repeats of the Ca^{2+} channel α_1-subunit, cooperate and form the high-affinity Ca^{2+} binding site that functions as selective filter in the multi-ion cardiac L-type Ca^{2+} channel [6, 25, 33]. The transient occupancy of the binding site by La^{3+}, Cd^{2+}, Co^{2+} and Mg^{2+}, inorganic Ca^{2+} channel blockers, induces short shut events in sustained single-channel Ba^{2+} currents in the presence of BAY K 8644, whereas Mn^{2+} produces shorter shut events as expected from its more rapid unbinding that is required for substantial permeation through the channel [19].

In papillary muscles from guinea-pig [35] and rat [1], Mn^{2+} produces an initial depression and a late augmentation of contractile force. The latter is contradictory to the blockade of Ca^{2+} channels. Acute depression of contractile function by infusion of Mn^{2+} in the Langendorff-perfused rat heart, with EC_{50} values for contractile indices of 120–250 μM [4], is explained by the blockade of slow Ca^{2+} current by Mn^{2+} with EC_{50} of 625 μM in rat ventricular muscle [30]. At 5 or 30 μM, Mn^{2+} hardly depresses the contractile function [4, 17]. However, low concentrations of Mn may affect myocardial functions within the cell. A 5 min infusion of 5 μM Mn^{2+} in the Langendorff-perfused rat heart induces an Mn uptake of ~100 nmol/kg wet weight and, furthermore, the uptake is augmented by isoproterenol as expected from the present increase of I_{Mn} [17]. In the presence of 20 nM Mn^{2+}, the concentration prevailing in human serum [36], Mn^{2+} uptake would require 21 h to reach that level, as Mn^{2+} influx is nearly proportional to the extracellular [Mn^{2+}] [4].

Transition metals, including Mn, are essential for many metabolic processes. For instance, manganese superoxide dismutase (SOD2), which converts superoxide to O_2 and H_2O_2, serves as the primary defence against mitochondrial oxidative stress that accelerates apoptosis in cardiac myocytes [38]. There exists a duality with Mn: while the element is crucial for proper cellular function, it is highly toxic if it accumulates above trace levels [26, 34]. The L-type Ca^{2+} channel is involved in the regulation of the intracellular [Mn]. Mn^{2+} that flows in through the opened L-type Ca^{2+} channels together with Ca^{2+} may eventually modulate the Ca^{2+}-induced cellular responses.

Acknowledgements This research was supported by the Science Research Promotion fund from the Promotion and Mutual Aid Corporation for Private Schools of Japan and grants from the Ministry of Education, Science, Sports, Culture and Technology of Japan and the Vehicle Racing Commemorative Foundation.

References

1. Agata N, Tanaka H, Shigenobu K (1992) Effect of Mn^{2+} on neonatal and adult rat heart: initial depression and late augmentation of contractile force. Eur J Pharmacol 222:223–226
2. Akaike N, Nishi K, Oyama Y (1983) Characteristics of manganese current and its comparison with currents carried by other divalent cations in snail soma membranes. J Membr Biol 76:289–297
3. Anderson M (1983) Mn ions pass through calcium channels. A possible explanation. J Gen Physiol 81:805–827
4. Brurok H, Schjøtt J, Karlsson JOG, Jynge P (1997) Manganese and the heart: acute cardiodepression and myocardial accumulation of manganese. Acta Physiol Scand 159:33–40
5. Eisenmann G, Horn R (1983) Ionic selectivity revisited: the role of kinetic and equilibrium processes in ion permeation through channels. J Membr Biol 76:197–225
6. Ellinor PT, Yang J, Sather WA, Zhang J-F, Tsien RW (1995) Ca^{2+} channel selectivity at a single locus for high-affinity Ca^{2+} interactions. Neuron 15:1121–1132
7. Findlay I (2002) Voltage- and cation-dependent inactivation of L-type Ca^{2+} channel currents in guinea-pig ventricular myocytes. J Physiol (Lond) 541:731–740
8. Frame MDS, Milanick MA (1991) Mn and Cd transport by the Na-Ca exchanger of ferret red blood cells. Am J Physiol 261:C467–C475
9. Fukuda J, Kawa K (1977) Permeation of manganese, cadmium, zinc, and beryllium through calcium channels of an insect muscle membrane. Science 196:309–311
10. Hadley RW, Lederer WJ (1992) Comparison of the effects of BAY K 8644 on cardiac Ca^{2+} current and Ca^{2+} channel gating current. Am J Physiol 262:H472–H477
11. Hagiwara S, Byerly L (1981) Calcium channel. Annu Rev Neurosci 4:69–125
12. Hamill OP, Marty A, Neher E, Sakmann B, Sigworth FJ (1981) Improved patch-clamp techniques for high-resolution current recording from cells and cell-free membrane patches. Pflügers Arch 391:85–100
13. Harvey RD, Hume JR (1989) Autonomic regulation of a chloride current in heart. Science 244:983–985
14. Hess P, Lansman JB, Tsien RW (1984) Different modes of Ca channel behavior favored by dihydropyridine Ca agonists and antagonists. Nature 311:538–544
15. Hess P, Lansman JB, Tsien RW (1986) Calcium channel selectivity for divalent and monovalent cations. Voltage and concentration dependence of single channel current in ventricular heart cells. J Gen Physiol 88:293–319
16. Hille B (2001) Ion channels of excitable membranes, 3rd edn. Sinauer, Sunderland, p 647
17. Hunter DR, Haworth RA, Berkoff, HA (1981) Cellular manganese uptake by the isolated perfused rat heart: a probe for the sarcolemma calcium channel. J Mol Cell Cardiol 13:823–832
18. Kawashima Y, Ochi R (1988) Voltage-dependent decrease in the availability of single calcium channels by nitrendipine in guinea-pig ventricular cells. J Physiol (Lond) 402:219–235
19. Lansman JB, Hess P, Tsien RW (1986) Blockade of current through single calcium channels by Cd^{2+}, Mg^{2+}, and Ca^{2+}. Voltage and concentration dependence of calcium entry into the pore. J Gen Physiol 88:321–347
20. Laurenza A, Sutkowski EM, Seamon KB (1989) Forskolin: a specific stimulator of adenylyl cyclase or a diterpene with multiple sites of action? Trends Pharmacol Sci 10:442–447
21. Lee KS, Tsien RW (1983) Mechanism of calcium channel blockade by verapamil, D600, diltiazem and nitrendipine in single dialyzed heart cells. Nature 302:790–794
22. Levesque PC, Hart PJ, Hume JR, Kenyon JL, Horowitz B (1992) Expression of cystic fibrosis transmembrane regulator Cl^- channels in heart. 71:1002–1007
23. McDonald TF, Pelzer S, Trautwein W, Pelzer DJ (1994) Regulation and modulation of calcium channels in cardiac, skeletal, and muscle cells. Physiol Rev 74:365–507
24. Monteilh-Zoller, MK, Hermosura MC, Nadler MJS, Scharenberg AM, Penner R, Fleig A (2003) TRP7 provides an ion channel mechanism for cellular entry of trace metal ions. J Gen Physiol 121:49–60
25. Mori Y, Mikala G, Varadi G, Kobayashi T, Koch S, Wakamori M, Schwarz A (1996) Molecular pharmacology of voltage-dependent calcium channels. Jpn J Pharmacol 72:83–109
26. Nelson N (1999) Metal ion transporters and homeostasis. EMBO J 18:4361–4371
27. Ochi R (1970) The slow inward current and the action of manganese ions in guinea-pigs myocardium. Pflügers Arch 316:81–94
28. Ochi R (1976) Manganese-dependent propagated action potentials and their depression by electrical stimulation in guinea-pig myocardium perused by sodium-free media. J Physiol (Lond) 263:139–156
29. Parekh AB, Penner R (1997) Store depletion and calcium current. Physiol Rev 77:901–930
30. Payet MD, Schamme OF, Ruiz-Cerette E, Deniers JM (1980) Inhibitory action of blockers of the slow inward current in rat myocardium, a study in steady state and of rate of action. J Mol Cell Cardiol 12:187–200
31. Physiological Society of Japan (1994) Guiding principles for the care and use of animals in the field of physiological sciences. Jpn J Physiol 44:5
32. Sanguinettei MC, Krafte DS, Kass RS (1986) Voltage-dependent modulation of Ca channel current in heart cells by Bay K 8644. J Gen Physiol 88:369–392
33. Sather WA, McClesky EW (2003) Permeation and Selectivity in Calcium channels. Annu Rev Physiol 65:133–159
34. Takeda A (2003) Manganese action in brain function. Brain Res Rev 41:79–87
35. Vierling W, Reiter M (1979) An intracellularly induced positive inotropic effect of manganese in guinea-pig ventricular myocardium. Naunyn-Schmiedeberg's Arch Pharmacol 306:249–253
36. Torra M, Rodamilans M, Corbella J (2002) Biological monitoring of environmental exposure to manganese in blood samples from residents of the city of Barcelona, Spain. Sci Total Environ 289:237–241
37. Uehara A, Hume JR (1985) Interactions of organic calcium channels in single frog atrial cells. J Gen Physiol 85:621–647
38. Van Remmen H, Williams MD, Guo Z, Estlack L, Yang H, Carlson EJ, Epstein CJ, Huang TT, Richardson A (2001) Knockout mice heterozygous for *Sod2* show alterations in cardiac mitochondrial function and apoptosis. Am J Physiol 281:H1422–H1432